J. Math. Anal. Appl. 534 (2024) 128051

Contents lists available at ScienceDirect

Journal of Mathematical Analysis and Applications

journal homepage: www.elsevier.com/locate/jmaa

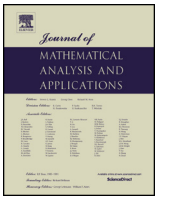

Regular Articles

An endeavor from the Glowinski-Le Tallec splitting for approximating the solution of Kawarada equation ☆

Qin Sheng

Department of Mathematics and Center for Astrophysics, Space Physics and Engineering Research, Baylor University, One Bear Place, Waco, TX 76798-7328, United States of America

ARTICLE INFO

Article history:
Received 29 May 2023
Available online 19 December 2023
Submitted by W. Layton

Keywords:
Operator splitting
Approximation order
Kawarada equations
Quenching blow-up
Finite difference methods
Stability

ABSTRACT

This paper studies an extended application of the Glowinski-Le Tallec splitting for approximating solutions of linear and nonlinear partial differential equations. It is shown that the three-level, six-component operator decomposition, originally designed for Lagrangian optimizations, provides a stable second-order operator splitting approximation for the solutions of evolutional partial differential equations. It is also found that the Glowinski-Le Tallec formula not only provides an effective enhancement to conventional two-level, four-component ADI and LOD methods, but also introduces a flexible way for constructing multi-parameter operator splitting strategies in respective spaces where broad spectrums of mathematical models may exist for important natural phenomena and applications. The extended operator splitting is utilized for solving a singular and nonlinear Kawarada problem satisfactorily. Multiple simulation results are presented.

1. Introduction

Splitting methods, with popular approaches such as alternating-direction implicit (ADI) and local one-dimensional (LOD) configurations [27,30,35], have been playing an irreplaceable role for approximating solutions of ordinary and partial differential equations in multiple physics applications. Their rich theoretical foundation including profound mathematical analysis can be traced back to Baker-Campbell-Hausdorff, Zassenhaus and Trotter formulas [4,10,22,32].

Needless to mention that classical splitting strategies have met an enormous amount of new challenges in recent years, especially due to emerging singular, stochastic and high-dimensional modeling problems from biomedical, engineering and deep neural network developments and simulations.

☆ The author is partially supported by the National Science Foundation Grant No. DMS-2318032; USA and Simons Foundation Grant No. MPS-1001466; USA.

E-mail address: qin_sheng@baylor.edu.

https://doi.org/10.1016/j.jmaa.2023.128051
0022-247X/

This paper focuses at an alternative operator splitting approach based on the Glowinski-Le Tallec formula which is traditionally used for approximating global solutions of equilibrium problems in Lagrangian optimizations [15,34]. The splitting structure exhibits an excellent parameter flexibility which is favorable in parallel computations and deep neural network designs for high dimensional problems. However, the Glowinski-Le Tallec strategy and its variants have traveled less often to territories of numerical solutions of differential equations. In this study, we shall analyze and show that the Glowinski-Le Tallec formula is in fact a highly vibrant second order approximation for solutions of evolutional equations that are fundamental in multiphysics applications. This order is optimal when linear and nonlinear diffusion equations are considered due to the Sheng-Suzuki accuracy barrier [8,29,31]. A two-dimensional singular and nonlinear Kawarada partial differential equation, which models solid fuel thermal combustion processes [1,18,19,28], will be used for experimenting with the Glowinski-Le Tallec splitting algorithm on anticipated stability that is crucial in mathematical approximations [9].

To commence, we consider the evolutional operator

$$P(A_1, A_2, \dots, A_N, t) = e^{-t(A_1+A_2+\cdots+A_N)}, \quad t > 0,$$

where $A_1, A_2 \dots, A_N \in \mathbb{R}^{m\times m},\ m \in \mathbb{N}^+$, and $[A_i, A_j] = A_iA_j - A_jA_i \neq O,\ i \neq j,\ 1 \leq i, j \leq N$. We intend to approximate $P(A_1, A_2, \dots, A_N, t)$ by a convex linear combination

$$Q(E_1, E_2, \dots, E_K, t) = \sum_{k=1}^{K} \gamma_k E_k, \tag{1.1}$$

where $\gamma_k \in \mathbb{R}^+$ being constant weights and $E_k,\ k = 1, 2, \dots, K$, are finite products of matrices $(I + \alpha_{k,\ell} t A_{r(k,\ell)})^{-1},\ (I - \beta_{k,\ell} t A_{r(k,\ell)}),\ r(k, \ell) \in \{1, 2, \dots, N\}$, with $\alpha_{k,\ell}, \beta_{k,\ell}$ being real constants. Interesting preliminary investigations for connections between operators P, Q can be found in [21,29]. We need the following.

Definition 1.1. [23,29] Assume that $t > 0$ be sufficiently small, that is, $0 < t \ll 1$. Then if the relation

$$\|P(A_1, A_2, \dots, A_N, t) - Q(E_1, E_2, \dots, E_K, t)\| = \mathcal{O}(t^{p+1}) \tag{1.2}$$

holds, we say that the approximation $Q(E_1, E_2, \dots, E_K, t)$ is accurate to the order p.

Definition 1.2. [16,29] An operator $R(t)$, such as P, Q, is stable in the norm $\|\cdot\|$ if there exists a uniform constant $C \in \mathbb{R}^+$, such that for $0 < t \ll 1$ and $nt \leq T$

$$\|R^n(t)\| \leq C$$

for all possible parameters used.

Lemma 1.3. [12] *For any $A \in \mathbb{R}^{m\times m}$ and positive parameter α, we have*

$$e^{-\alpha\mu(A)} \leq \left\|e^{-\alpha A}\right\| \leq e^{\alpha\mu(-A)},$$

where $\mu(A)$ is the logarithmic norm of A.

Lemma 1.4. *If for all eigenvalues λ of $A_1, A_2, \dots, A_N$ we have $\mathrm{Re}(\lambda) \geq 0$, then the matrix exponential operator $P(A_1, A_2, \dots, A_N, t)$ is stable.*

Proof. This is a straightforward deduction from Lemma 1.3. □

Let $\mathbb{H}$ be a normed space and $\mathcal{D} \subset \mathbb{H}$ be nonempty convex set, and let f be a function $\mathcal{D} \times \mathcal{D} \to \mathbb{R}$ such that $f(x,x) = 0$ for $x \in \mathcal{D}$. The function $(x,\cdot) : \mathcal{D} \to \mathbb{R}$ is assumed to be convex and differentiable at $x \in \mathcal{D}$. An equilibrium optimization problem associated with f is the following:

$$\text{to find } x^* \in \mathcal{D} \subset \mathbb{H} \text{ such that } f(x^*, y) \geq 0 \text{ for all } y \in \mathcal{D}.$$

The set of solutions of the equilibrium problem should be nonempty [34]. If for $x \in \mathcal{D}$ we set $N_{\mathcal{D}}(x) = Ax$, $\nabla f(x,x) = Bx$, where $N_{\mathcal{D}}(x)$ is the normal cone to $\mathcal{D}$ at x, then the operators A, B may be maximal monotones and A, B do not, in general, commute [2]. In the circumstance, the underlying equilibrium problem becomes equivalent to [34]:

$$\text{to find } x^* \in \mathcal{D} \subset \mathbb{H} \text{ such that } 0 \in Ax^* + Bx^*. \tag{1.3}$$

The traditional forward-backward iterative procedure for solving the optimization problem (1.3) is

$$x^{(k+1)} = J_{\lambda_0 A}(I - \lambda_0 tB)x^{(k)}, \quad k = 0, 1, 2, \ldots; \ t > 0,$$

where $\lambda_0 t > 0$ is some stepsize chosen, I is the identity operator, and $J_{\lambda_0 A} = (I + \lambda_0 tA)^{-1}$ is a resolvent operator of A. Investigations of the convergence of such $x^{(k)}$ to x^* as $k \to \infty$ can be found in numerous recent publications (for instance, see [15,24,34] and references therein).

The Glowinski-Le Tallec splitting is an operator iterative procedure equipped with three resolvent operators, that is,

$$x^{(k+1)} = G(A, B, \lambda_1, \lambda_2, t)x^{(k)}, \quad k = 0, 1, 2, \ldots; \ t > 0,$$

where G is a triple level and six-component decomposition formula with dual parameters,

$$\begin{aligned} G(A, B, \lambda_1, \lambda_2, t) &= J_{\lambda_1 tA}(I - \lambda_1 tB)J_{\lambda_2 tB}(I - \lambda_2 tA)J_{\lambda_1 tA}(I - \lambda_1 tB) \\ &= (I + \lambda_1 tA)^{-1}(I - \lambda_1 tB)(I + \lambda_2 tB)^{-1}(I - \lambda_2 tA)(I + \lambda_1 tA)^{-1}(I - \lambda_1 tB) \\ &= H(A, B, \lambda_1, \lambda_2, t)(I + \lambda_1 tA)^{-1}(I - \lambda_1 tB), \quad t > 0, \end{aligned} \tag{1.4}$$

where $H(A, B, \lambda_1, \lambda_2, t) = (I + \lambda_1 tA)^{-1}(I - \lambda_1 tB)(I + \lambda_2 tB)^{-1}(I - \lambda_2 tA)$, $\lambda_1, \lambda_2, t \in \mathbb{R}^+$.

Now, let us set $N = 2$ in operators P and Q. Denote $A = A_1$, $B = A_2$. Further, let $A, B \in \mathbb{R}^{m \times m}$ and assume that $[A, B] = AB - BA \neq O$. We wish to see if the Glowinski-Le Tallec splitting formulas G, H defined in (1.4) offer consistent approximations to the matrix exponential P which is the key to the solution of evolution equations.

We also wish to find out possible connections between G, H and the traditional two-level, four-component ADI operator

$$\tilde{Q}(A, B, t) = (I + (t/2)A)^{-1}(I - (t/2)B)(I + (t/2)B)^{-1}(I - (t/2)A), \quad 0 < t \ll 1,$$

as well as the standard two-level, four-component LOD operator

$$\hat{Q}(A, B, t) = (I - (t/2)A)(I + (t/2)A)^{-1}(I - (t/2)B)(I + (t/2)B)^{-1}, \quad 0 < t \ll 1,$$

for approximating the matrix exponential evolutional operator $P(A, B, t) = e^{-t(A+B)}$ [8,11,23,30,35]. Note that both ADI and LOD operators are second order approximations to the operator P. Thus, it is natural

that we may wish to verify if G and H may provide similar accuracies with additional flexibility in parameter selections for favorable programming realizations. The studies can be viewed as a continuation of the pioneering work by P. L. Lions and B. Mercier [21].

2. Order of accuracy

Let the parameter $\lambda \in \mathbb{R}^+$ and A, B do not commute. Similar to [21], utilizing Taylor series expansions we have

$$\begin{aligned}
(I+\lambda tA)^{-1}(I-\lambda tB) &= (I-\lambda tA+\lambda^2t^2A^2-\lambda^3t^3A^3+\lambda^4t^4A^4-\cdots)(I-\lambda tB)\\
&= I-\lambda t(A+B)+\lambda^2t^2(A^2+AB)-\lambda^3t^3(A^3+A^2B)\\
&\quad +\lambda^4t^4(A^4+A^3B)-\cdots,\\
(I+\lambda tB)^{-1}(I-\lambda tA) &= (I-\lambda tB+\lambda^2t^2B^2-\lambda^3t^3B^3+\lambda^4t^4B^4-\cdots)(I-\lambda tA)\\
&= I-\lambda t(B+A)+\lambda^2t^2(B^2+BA)-\lambda^3t^3(B^3+B^2A)\\
&\quad +\lambda^4t^4(B^4+B^3A)-\cdots.
\end{aligned}$$

It follows immediately that

$$\begin{aligned}
H(A,B,\lambda_1,\lambda_2,t) &= (I+\lambda_1tA)^{-1}(I-\lambda_1tB)(I+\lambda_2tB)^{-1}(I-\lambda_2tA)\\
&= \left[I-\lambda_1t(A+B)+\lambda_1^2t^2(A^2+AB)-\lambda_1^3t^3(A^3+A^2B)+\lambda_1^4t^4(A^4+A^3B)-\cdots\right]\\
&\quad\times\left[I-\lambda_2t(B+A)+\lambda_2^2t^2(B^2+BA)-\lambda_2^3t^3(B^3+B^2A)+\lambda_2^4t^4(B^4+B^3A)-\cdots\right]\\
&= I-(\lambda_1+\lambda_2)t(A+B)+t^2\left[(\lambda_1^2+\lambda_1\lambda_2)A^2+(\lambda_1^2+\lambda_1\lambda_2)AB+(\lambda_1\lambda_2+\lambda_2^2)BA\right.\\
&\quad\left.+(\lambda_1\lambda_2+\lambda_2^2)B^2\right]-t^3\left[(\lambda_1^2\lambda_2+\lambda_1^3)A^3+(\lambda_1^2\lambda_1+\lambda_1^3)A^2B+(\lambda_1\lambda_2^2+\lambda_1^2\lambda_2)ABA\right.\\
&\quad\left.+(\lambda_1\lambda_2^2+\lambda_2^3)B^2A+(\lambda_1\lambda_2^2+\lambda_1^2\lambda_2)AB^2+(\lambda_1\lambda_2^2+\lambda_2^3)B^3\right]+\cdots.
\end{aligned}$$

Furthermore,

$$\begin{aligned}
G(A,B,\lambda_1,\lambda_2,t) &= H(A,B,\lambda_1,\lambda_2,t)(I+\lambda_1tA)^{-1}(I-\lambda_1tB)\\
&= H(A,B,\lambda_1,\lambda_2,t)\left[I-\lambda_1t(A+B)+\lambda_1^2t^2(A^2+AB)-\lambda_1^3t^3(A^3+A^2B)\right.\\
&\quad\left.+\lambda_1^4t^4(A^4+A^3B)-\cdots\right]\\
&= I-t(2\lambda_1+\lambda_2)(A+B)+t^2\left[(3\lambda_1^2+2\lambda_1\lambda_2)A^2+(3\lambda_1^2+2\lambda_1\lambda_2)AB\right.\\
&\quad\left.+(\lambda_1^2+2\lambda_1\lambda_2+\lambda_2^2)BA+(\lambda_1^2+2\lambda_1\lambda_2+\lambda_2^2)B^2\right]-t^3\left\{(4\lambda_1^3+2\lambda_1^2\lambda_2)A^3\right.\\
&\quad+(3\lambda_1^3+3\lambda_1^2\lambda_2)A^2B+(\lambda_1^3+2\lambda_1^2\lambda_2+\lambda_1\lambda_2^2)ABA+(\lambda_1^3+2\lambda_1^2\lambda_2+\lambda_1\lambda_2^2)BA^2\\
&\quad+(\lambda_1^3+2\lambda_1^2\lambda_2+\lambda_1\lambda_2^2)BAB+(\lambda_1^2\lambda_2+2\lambda_1\lambda_2^2+\lambda_2^3)B^2A+(\lambda_1^3+2\lambda_1^2\lambda_2+\lambda_1\lambda_2^2)AB^2\\
&\quad\left.+(\lambda_1^2\lambda_2+2\lambda_1\lambda_2^2+\lambda_2^3)B^3\right\}+\cdots \qquad (2.1)
\end{aligned}$$

Theorem 2.1. *If* $\lambda_1=\left(2-\sqrt{2}\right)/2,\ \lambda_2=-1+\sqrt{2}$ *then*

$$\left\|G(A,B,\lambda_1,\lambda_2,t)-e^{-t(A+B)}\right\|=\mathcal{O}(t^3),\quad t\to 0^+,$$

where $\|\cdot\|$ *is any suitable matrix norm. Therefore* $G(A,B,\lambda_1,\lambda_2,t)$ *is a second order stable operator splitting formula. The selection of such nonnegative* λ_1,λ_2 *is unique.*

Proof. Note that

$$\begin{aligned} e^{-t(A+B)} &= I - t(A+B) + \frac{t^2}{2}(A+B)^2 - \frac{t^3}{3!}(A+B)^3 + \cdots \\ &= I - t(A+B) + \frac{t^2}{2}A^2 + \frac{t^2}{2}AB + \frac{t^2}{2}BA + \frac{t^2}{2}B^2 - \frac{t^3}{3!}A^3 - \frac{t^3}{3!}A^2B \\ &\quad -\frac{t^3}{3!}ABA - \frac{t^3}{3!}BA^2 - \frac{t^3}{3!}AB^2 - \frac{t^3}{3!}BAB - \frac{t^3}{3!}B^2A - \frac{t^3}{3!}B^3 + \cdots . \end{aligned} \tag{2.2}$$

Recall (2.1). We may set

$$2\lambda_1 + \lambda_2 = 1, \tag{2.3}$$

$$3\lambda_1^2 + 2\lambda_1\lambda_2 = \frac{1}{2}, \tag{2.4}$$

$$\lambda_1^2 + 2\lambda_1\lambda_2 + \lambda_2^2 \;=\; (\lambda_1+\lambda_2)^2 = \frac{1}{2}. \tag{2.5}$$

From (2.3) we have $\lambda_2 = 1 - 2\lambda_1$. A substitution of the result into (2.5) yields

$$(\lambda_1 + 1 - 2\lambda_1)^2 = (1-\lambda_1)^2 = \frac{1}{2}.$$

Therefore

$$\lambda_1 = 1 \mp \frac{\sqrt{2}}{2},\ \lambda_2 = -1 \pm \sqrt{2}.$$

Substitute the above to (2.4). We acquire that

$$\begin{aligned} 3\lambda_1^2 + 2\lambda_1\lambda_2 &= 3\left(1 \mp \frac{\sqrt{2}}{2}\right)^2 + 2\left(1 \mp \frac{\sqrt{2}}{2}\right)\left(-1 \pm \sqrt{2}\right) \\ &= 3\left(1 \mp \sqrt{2} + \frac{1}{2}\right) + 2\left(-1 \pm \sqrt{2} \pm \frac{\sqrt{2}}{2} - 1\right) \;=\; \frac{1}{2}. \end{aligned}$$

Since for the stability parameters λ_1, λ_2 must maintain their positivity [8,23,29], thus, $\lambda_1 = 1 - \frac{\sqrt{2}}{2},\ \lambda_2 = -1 + \sqrt{2}$. On the other hand, for such λ_1, λ_2 we have

$$4\lambda_1^3 + 2\lambda_1^2\lambda_2 = 2\lambda_1^2(2\lambda_1 + \lambda_2) = 2\left(\frac{3}{2} - \sqrt{2}\right)\left(2 - \sqrt{2} - 1 + \sqrt{2}\right) = 3 - 2\sqrt{2} \;\neq\; \frac{1}{6}.$$

Compare the above with (2.2). We know immediately that the maximal order of accuracy for a stable approximation is $p = 2$ and thus the theorem is true. □

Corollary 2.2. *If $\lambda_1 = \lambda_2 = 1/2$ then*

$$\left\| H(A,B,\lambda_1,\lambda_2,t) - e^{-t(A+B)} \right\| = \mathcal{O}(t^3), \quad t \to 0^+,$$

where $\|\cdot\|$ is any suitable matrix norm. Therefore $H(A,B,1/2,1/2,t)$ is a second order stable operator splitting formula. The selection of such nonnegative λ_1, λ_2 is unique.

Proof. Recall that

$$\begin{aligned}H(\lambda_1,\lambda_2,t,A,B) = I-(\lambda_1+\lambda_2)t(A+B)+t^2\left[(\lambda_1^2+\lambda_1\lambda_2)A^2+(\lambda_1^2+\lambda_1\lambda_2)AB\right.\\ \left.+(\lambda_1\lambda_2+\lambda_2^2)BA+(\lambda_1\lambda_2+\lambda_2^2)B^2\right]-t^3\left[(\lambda_1^2\lambda_2+\lambda_1^3)A^3+(\lambda_1^2\lambda_1+\lambda_1^3)A^2B\right.\\ \left.+(\lambda_1\lambda_2^2+\lambda_1^2\lambda_2)ABA+(\lambda_1\lambda_2^2+\lambda_2^3)B^2A+(\lambda_1\lambda_2^2+\lambda_1^2\lambda_2)AB^2+(\lambda_1\lambda_2^2+\lambda_2^3)B^3\right]+\cdots.\end{aligned}$$

Thus, to ensure that $H(A,B,\lambda_1,\lambda_2,t)$ is a second order approximation, we must need

$$\lambda_1+\lambda_2=1, \tag{2.6}$$

$$\lambda_1^2+\lambda_1\lambda_2=\frac{1}{2}, \tag{2.7}$$

$$\lambda_1\lambda_2+\lambda_2^2=\frac{1}{2}. \tag{2.8}$$

Again, from (2.6) we have $\lambda_2=1-\lambda_1$. A substitution of it to (2.7) leads to

$$\lambda_1=\lambda_2=\frac{1}{2}$$

which satisfies naturally (2.8). Further, we observe that

$$\lambda_1^2\lambda_2+\lambda_1^3=\lambda_1^2(\lambda_2+\lambda_1)=\frac{1}{4}\neq\frac{1}{6}.$$

Therefore $p=2$ and H is the only second order stable approximation to $P(A,B,t)=e^{-t(A+B)},\ t\to 0^+$. □

Remark 2.3. Though the nonpositive pair of parameters $\lambda_1=\left(2+\sqrt{2}\right)/2,\ \lambda_2=-1-\sqrt{2}$ cannot be used for solving diffusion partial differential equations due to instability concerns [4,22,29,30], it may be employed for decomposed solutions of other types of equations such as linear and nonlinear fluid equations. Careful additional explorations are thus needed.

Remark 2.4. The four-component splitting operator $H(A,B,1/2,1/2,t)$ is identical to the traditional ADI operator $\tilde{Q}(A,B,t)$ as $t\to 0^+$.

3. Application to a Kawarada problem

Let $\sigma\in\mathbb{R}^+,\ \mathcal{D}=(0,1)\times(0,1)$ be a squared physical domain with boundary $\partial\mathcal{D}$, and $\bar{\mathcal{D}}=\mathcal{D}\cup\partial\mathcal{D}$. We consider following nonlinear Kawarada advection-diffusion problem [14,17,18],

$$\sigma^2 w_t=\nabla(\alpha\nabla w)+\sigma^2\phi(w),\quad (x,y)\in\mathcal{D},\ t>0, \tag{3.1}$$

$$w(x,y,t)=0,\quad (x,y)\in\partial\mathcal{D},\ t\geq 0, \tag{3.2}$$

$$w(x,y,0)=w_0(x,y),\quad (x,y)\in\mathcal{D}, \tag{3.3}$$

where $\nabla=(\partial_x,\partial_y)^\intercal,\ \alpha(x,y)>0$ is differentiable for $(x,y)\in\mathcal{D}$, and $0<w_0(x,y)\ll\theta\in\mathbb{R}^+$. The nonlinear source function, $\phi(w)$, is strictly increasing for $0\leq w<\theta$ with

$$\phi(0)=\phi_0>0,\quad \lim_{\max(w)\to\theta^-}\phi(w)=\infty.$$

Investigations of the existence, uniqueness and intriguing properties of the solution of (3.1)-(3.3) can be found in many recent publications including [6,18,19,25]. In the context of solid propellant combustion, the function $w(x,y,t)$ represents the temperature distribution in an idealized chamber, and x and y are coordinates in the perpendicular and parallel directions to its walls, respectively. The value of θ is often referred to as the fuel ignition temperature in combustion, or the critical point for a massive corrosion to occur in a container. We say that a solution $w(x,y,t)$ quenches if there exist $(\tilde{x},\tilde{y}) \in \bar{\mathcal{D}}$ and $\tilde{t} < \infty$ such that $w(x,y,t) \to \theta^-$ as $(x,y) \to (\tilde{x},\tilde{y}), t \to \tilde{t}^-$. It has been shown that θ exists only when $\sigma > \sigma^* > 0$ [1,14,28]. The particular value σ^* is often referred to as the critical size in thermal engineering and combustion applications [6,18,19,28].

Let $m \in \mathbb{N}^+$ be sufficiently large and $h = 1/(m+1)$. We define uniform mesh regions $\mathcal{D}_h = \{(x_i,y_j) \mid x_i = ih, y_j = jh,\ 1 \le i,j \le m\}$ and $\bar{\mathcal{D}}_h = \{(x_i,y_j) \mid x_i = ih, y_j = jh,\ 0 \le i,j \le m+1\}$ on $\bar{\mathcal{D}}$. Assume that $w_{i,j}$ be an approximation of the solution w at $(x_i,y_j) \in \bar{\mathcal{D}}_h$. Utilizing conventional recursive central finite differences approximating the spatial derivatives, we obtain the following semi-discretized system from (3.1):

$$\begin{aligned}(w_t)_{i,j} = \frac{1}{\sigma^2 h^2}\big[&\alpha_{i-1/2,j}w_{i-1,j} + \alpha_{i+1/2,j}w_{i+1,j} - (\alpha_{i-1/2,j} + \alpha_{i+1/2,j})w_{i,j}\\ &+ \alpha_{i,j-1/2}w_{i,j-1} + \alpha_{i,j+1/2}w_{i,j+1} - (\alpha_{i,j-1/2} + \alpha_{i,j+1/2})w_{i,j}\big] + \phi(w_{i,j}),\quad 1 \le i,j \le m.\end{aligned}$$

Denote $w = (w_{1,1}, w_{2,1}, w_{3,1}, \dots, w_{N,1}, w_{1,2}, \dots, w_{m,m})^\intercal \in \mathbb{R}^{m^2}$ based on a natural ordering [16]. The semi-discretized system for solving (3.1)-(3.3) can be comprised to yield

$$w' = (A+B)w + \phi(w), \quad t > 0, \tag{3.4}$$

$$w(0) = w_0, \tag{3.5}$$

in which

$$\begin{aligned}&A = \frac{1}{\sigma^2 h^2}\mathrm{diag}\left(A_1, A_2, \dots, A_m\right),\ B = \frac{1}{\sigma^2 h^2}\mathrm{tridiag}\left(B_j^1, B_j^2, B_j^3\right) \in \mathbb{R}^{m^2 \times m^2},\\ &\phi(w) = [\phi(w_{1,1}), \phi(w_{2,1}), \dots, \phi(w_{m,1}), \phi(w_{1,2}), \phi(w_{2,2}), \dots, \phi(w_{m,m})]^\intercal \in \mathbb{R}^{m^2},\\ &w_0 = [(w_0)_{1,1}, (w_0)_{2,1}, \dots, (w_0)_{m,1}, (w_0)_{1,2}, (w_0)_{2,2}, \dots, (w_0)_{m,m}]^\intercal \in \mathbb{R}^{m^2},\end{aligned}$$

where $A_j \in \mathbb{R}^{m\times m}$, $1 \le j \le m$, are tridiagonal matrices with upper, lower and diagonal entries respectively being

$$\begin{aligned}&u_{i,j} = \alpha_{i+1/2,j},\ i = 1,2,\dots,m-1,\\ &\ell_{i,j} = \alpha_{i-1/2,j},\ i = 2,3,\dots,m,\\ &d_{i,j} = -\alpha_{i-1/2,j} - \alpha_{i+1/2,j},\ i = 1,2,\dots,m,\end{aligned}$$

and B_j^1, B_j^2, and $B_j^3 \in \mathbb{R}^{m\times m}$ are diagonal matrices given by

$$\begin{aligned}&B_j^1 = \mathrm{diag}\left(\alpha_{i,j-1/2}\right),\ i = 1,2,\dots,m,\ j = 2,3,\dots,m,\\ &B_j^2 = -\mathrm{diag}\left(\alpha_{i,j-1/2} + \alpha_{i,j+1/2}\right),\ i = 1,2,\dots,m,\ j = 1,2,\dots,m,\\ &B_j^3 = \mathrm{diag}\left(\alpha_{i,j+1/2}\right),\ i = 1,2,\dots,m,\ j = 1,2,\dots,m-1.\end{aligned}$$

It can be observed in above configurations that matrices A, B are symmetric regardless types of the diffusion function $\alpha(x,y) > 0$ used. The matrices are also diagonally dominant and thus negative definite. These properties offer desirable potentials and convenience for applications of the splitting methods.

The formal solution of (3.4), (3.5) can be expressed as

$$w(t) = e^{t(A+B)}w_0 + \int_0^t e^{(t-\xi)(A+B)}\phi(w)d\xi, \quad 0 \le t \le T_\sigma, \tag{3.6}$$

where $T_\sigma < \infty$ is the finite quenching time corresponding to $\sigma \ge \sigma^*$ [14,16,20].

Consider the variable step temporal grids $\{t_0, t_1, t_2, \ldots, t_{N_\sigma+1}\}$, in which $t_0 = 0,\ t_{n+1} = t_n + \tau_n$ with variable temporal steps $0 < \tau_n \ll 1,\ n = 0, 1, 2, \ldots, N_\sigma$, and $t_{N_\sigma+1} = T_\sigma$. Note that values of τ_n can be determined via a proper adaptive mechanism, such as the moving mesh method [7]. A weak Courant constraint κ_n is considered under the tolerance $0 \le \epsilon < 1$: $\kappa_n = \tau_n/h^2 \in [\kappa-\epsilon, \kappa+\epsilon],\ n = 0, 1, 2, \ldots, N_\sigma;\ \kappa \in \mathbb{R}^+$. The terminal index N_σ depends on σ and therefore T_σ. Thus (3.6) can be reformulated to

$$w(t_{n+1}) = e^{\tau_n(A+B)}w(t_n) + \int_{t_n}^{t_{n+1}} e^{(t_{n+1}-\xi)(A+B)}\phi(w)d\xi, \quad n = 0, 1, \ldots, N_\sigma < \infty. \tag{3.7}$$

Denote w^n as an approximation of $w(t_n),\ n = 0, 1, 2, \ldots, N_\sigma + 1$. Based on the triple level Glowinski-Le Tallec splitting formula $G(A, B, \lambda_1, \lambda_2, t)$ defined in (1.4) with $\lambda_1 = 1 - \sqrt{2}/2, \lambda_2 = \sqrt{2} - 1$, we acquire the following second order trapezoid rule based implicit scheme from (3.7),

$$\begin{aligned} w^{n+1} &= (I - \lambda_1\tau_n A)^{-1}(I + \lambda_1\tau_n B)(I - \lambda_2\tau_n B)^{-1}(I + \lambda_2\tau_n A)(I - \lambda_1\tau_n A)^{-1}(I + \lambda_1\tau_n B) \\ &\quad \times \left(w^n + \frac{\tau_n}{2}\phi(w^n)\right) + \frac{\tau_n}{2}\phi(w^{n+1}), \quad n = 0, 1, \ldots, N_\sigma, \\ w^0 &= w_0. \end{aligned}$$

The above algorithm is highly nonlinear. To solve, proper iterative strategies are often needed. However, since we wish to focus at the applicability of (1.4), we may simply replace $\phi(w^{n+1})$ by $\phi(\hat{w}^{n+1})$, where the solution vector $\hat{w}^{n+1}$ is preevaluated via an explicit integrator such as a two-stage Runge-Kutta formula, or the three-stage Nyström scheme. Under such configuration, our Glowinski-Le Tallec splitting scheme can be linearized to yield following semi-adaptive implicit method,

$$\begin{aligned} w^{n+1} &= (I - \lambda_1\tau_n A)^{-1}(I + \lambda_1\tau_n B)(I - \lambda_2\tau_n B)^{-1}(I + \lambda_2\tau_n A)(I - \lambda_1\tau_n A)^{-1}(I + \lambda_1\tau_n B) \\ &\quad \times \left(w^n + \frac{\tau_n}{2}\phi(w^n)\right) + \frac{\tau_n}{2}\phi(\hat{w}^{n+1}), \quad n = 0, 1, \ldots, N_\sigma, \end{aligned} \tag{3.8}$$

$$w^0 = w_0. \tag{3.9}$$

We may notice the sign changes in (3.8) due to the matrix exponential to approximate is now $\exp\{\tau_n(A + B)\}$. Among the many important characteristic features of (3.1)-(3.3) and its solution approximations through (3.8), (3.9), a key issue to investigate is the stability of the Glowinski-Le Tallec method (3.8), (3.9) in the von Neumann sense, since it ensures required localized stability and convergence as $h \to 0^+$ [3,7,9,16,33]. To this end, we recall the fact that $A, B \in \mathbb{R}^{m^2\times m^2}$ are negative definite. The following results become thus straightforward.

Lemma 3.1. [17] *We have*

$$\|A\|_2,\ \|B\|_2 \le \frac{4}{\sigma^2 h^2} \max_{(x,y)\in\bar{\mathcal{D}}} \alpha(x, y).$$

Lemma 3.2. *If*

$$\kappa_n = \frac{\tau_n}{h^2} < \frac{\sigma^2}{2\lambda_2 \max_{i,j}\left\{\alpha_{i\pm1/2,j}, \alpha_{i,j\pm1/2}\right\}} \tag{3.10}$$

then

$$\left\|I + \tau_n\lambda_2 A\right\|_2, \ \left\|I + \tau_n\lambda_1 B\right\|_2, \ \left\|(I - \tau_n\lambda_1 A)^{-1}\right\|_2, \ \left\|(I - \tau_n\lambda_2 B)^{-1}\right\|_2 \le 1.$$

Proof. We first notice that

$$\left\|I + \tau_n\lambda_2 A\right\|_2 = \rho\left(I + \tau_n\lambda_2 A\right)$$

which is the spectrum radius of the matrix. We further observe that the eigenvalue of the matrix, $\lambda\left(I + \tau_n\lambda_2 A\right) = 1 + \tau_n\lambda_2\lambda(A) < 1$, since eigenvalues of A are real and negative.

Now, recall Lemma 3.1. We find that

$$1 + \tau_n\lambda_2\lambda(A) > 1 - \frac{4\tau_n\lambda_2}{\sigma^2 h^2}\max_{i,j}\left\{\alpha_{i\pm1/2,j}, \alpha_{i,j\pm1/2}\right\} > -1$$

due to the lemma hypothesis. The above implies that $\left\|I + \tau_n\lambda_2 A\right\| = \rho\left(I + \tau_n\lambda_2 A\right) \le 1$. Similarly, we can show that $\left\|I + \tau_n\lambda_1 B\right\| \le 1$ since A, B are similar and $\lambda_2 > \lambda_1 > 0$.

Secondly, we consider the spectrum radius of the matrix $(I - \tau_n\lambda_1 A)^{-1}$. Since it is symmetric, we have

$$\left\|(I - \tau_n\lambda_1 A)^{-1}\right\|_2 = \rho\left((I - \tau_n\lambda_1 A)^{-1}\right) = \frac{1}{\min_\lambda\left(1 - \tau_n\lambda_1\lambda(A)\right)} < 1$$

due to the fact again that A is negative definite. For the same reason the above inequality must be true. □

Definition 3.3. [13,16] Let the perturbed system corresponding to a numerical method such as (3.8), (3.9) be

$$\epsilon^{n+1} = M\epsilon^n, \quad n = 0, 1, \ldots,$$

where $\epsilon^\ell = w^\ell - \tilde{w}^\ell$, $\tilde{w}^\ell$ is a perturbed solution at the temporal level ℓ, $\ell = 0, 1, \ldots$, and M is the perturbed coefficient matrix. We say that the numerical method is stable in the norm $\|\cdot\|$ if there exists a uniform constant $c_0 \in \mathbb{R}^+$, such that for $\tau = \max_{\ell\in\mathbb{N}^+}\tau_\ell \to 0^+$

$$\left\|\epsilon^{n+1}\right\| \le c_0\left\|\epsilon^0\right\|, \quad n = 0, 1, \ldots.$$

Theorem 3.4. *If the hypothesis* (3.10) *holds and the spectral norm of the Jacobian* $\phi'(w)$ *is uniformly bounded, then the linearized semi-adaptive Glowinski-Le Tallec splitting method* (3.8), (3.9) *is weakly stable in the spectral norm and von Neumann sense.*

Proof. Let $\tilde{w}^n, \tilde{w}^{n+1}$ be perturbed solution vectors of (3.8), that is,

$$\begin{aligned}\tilde{w}^{n+1} = {} & (I - \lambda_1\tau_n A)^{-1}(I + \lambda_1\tau_n B)(I - \lambda_2\tau_n B)^{-1}(I + \lambda_2\tau_n A)(I - \lambda_1\tau_n A)^{-1}(I + \lambda_1\tau_n B) \\ & \times\left(\tilde{w}^n + \frac{\tau_n}{2}\phi(\tilde{w}^n)\right) + \frac{\tau_n}{2}\phi(\hat{w}^{n+1}), \quad n \in \{0, 1, \ldots, N_\sigma\}.\end{aligned}$$

Thus,

$$\begin{aligned}\varepsilon^{n+1} &= w^{n+1} - \tilde{w}^{n+1} = (I-\lambda_1\tau_n A)^{-1}(I+\lambda_1\tau_n B)(I-\lambda_2\tau_n B)^{-1}(I+\lambda_2\tau_n A)\\ &\quad\times(I-\lambda_1\tau_n A)^{-1}(I+\lambda_1\tau_n B)\left(w^n-\tilde{w}^n+\frac{\tau_n}{2}(\phi(w^n)-\phi(\tilde{w}^n)\right)\\ &= (I-\lambda_1\tau_n A)^{-1}(I+\lambda_1\tau_n B)(I-\lambda_2\tau_n B)^{-1}(I+\lambda_2\tau_n A)\\ &\quad\times(I-\lambda_1\tau_n A)^{-1}(I+\lambda_1\tau_n B)\left(I+\frac{\tau_n}{2}\phi'(\zeta^n)\right)\varepsilon^n, \quad n\in\{0,1,\ldots,N_\sigma\},\end{aligned}$$

where the vector ζ^n is between w^n and $\tilde{w}^n$.

Now, let $\|\phi'(\zeta^n)\|_2 \le 2c$ for some $c>0,\ \tau_n\le\tau\ll 1,\ n=0,1,\ldots,N_\sigma$. It follows from the above that

$$\begin{aligned}\left\|\varepsilon^{n+1}\right\|_2 &\le \left\|(I-\lambda_1\tau_n A)^{-1}(I+\lambda_1\tau_n B)(I-\lambda_2\tau_n B)^{-1}(I+\lambda_2\tau_n A)\right.\\ &\quad\left.\times\,(I-\lambda_1\tau_n A)^{-1}(I+\lambda_1\tau_n B)\right\|_2\left\|I+\frac{\tau_n}{2}\phi'(\zeta^n)\right\|_2\|\varepsilon^n\|_2\\ &\le \left(1+\frac{\tau_n}{2}\|\phi'(\zeta^n)\|_2\right)\|\varepsilon^n\|_2 \;=\; (1+c\tau)\|\varepsilon^n\|_2, \quad n\in\{0,1,\ldots,N_\sigma\}.\end{aligned}$$

Recursively we obtain that

$$\left\|\varepsilon^{n+1}\right\|_2 \le (1+c\tau)^n\left\|\varepsilon^0\right\|_2 = (1+c\tau)^{(1/c\tau)\tilde{N}_\sigma c}\left\|\varepsilon^0\right\|_2,$$

since $n=\tilde{N}_\sigma/\tau$, the value $\tilde{N}_\sigma\approx N_\sigma$ which is finite and decided solely by the quenching size $\sigma>\sigma^*>0$ [1,3,6]. Therefore

$$\left\|\varepsilon^{n+1}\right\|_2 \le \exp\left\{\tilde{N}_\sigma c\right\}\left\|\varepsilon^0\right\|_2 = c_0\left\|\varepsilon^0\right\|_2, \quad 0<\tau\ll 1.$$

Hence our proof is completed based on Definition 3.3. □

Remark 3.5. We may notice that Definition 3.3 is in fact a direction extension of Definition 1.2 for discretized evolutional operators when $\tau\to 0^+$.

Based on the accuracy of the Glowinski-Le Tallec splitting, recursive spatial difference formula and weak Courant constraint used, we may predict that the order of convergence for (3.8), (3.9) is linear in time. Although a rigorous proof of such argument is extremely difficult in our circumstance, primarily due to the strong quenching nonlinearity and singularity of the Kawarada problem [11,25,28], computational assessments of the convergence are possible through the Milne device [16,17]. More detailed discussions will follow in the next section.

4. Simulation experiments

Consider the nonlinear Kawarada initial-boundary value problem (3.1)-(3.3). We adopt modeling functions and parameters,

$$\alpha(x,y)=\exp\left\{-d\left[\left(x-\frac{1}{2}\right)^2+\left(y-\frac{1}{2}\right)^2\right]\right\},\ \phi(w)=\frac{1}{\theta-w},\ w_0(x,y)=\epsilon\sin^4(\kappa_1\pi x)\sin^4(\kappa_2\pi y),$$

where $d=10,\ \theta=1,\ \epsilon=1/100,\ \kappa_1,\kappa_2\in\mathbb{N}^+,\ (x,y)\in\mathcal{D}$ with $\sigma=\pi$. These functions and parameters are typical for stability validation experiments. They are used frequently in recent quenching modeling and investigations [3,7,17,20,25]. The use of κ_1,κ_2 reflects a possible installation of multiple sparking ignition systems, though the single point quenching profile remains unchanged [1,25,28]. For the simplicity of discussions, we take $\kappa_1=1,\kappa_2=2$ throughout continuing simulation experiments. Algorithms based

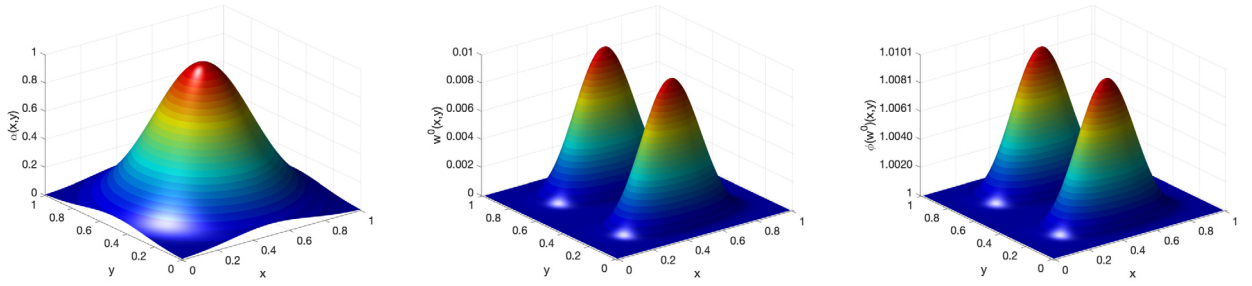

Fig. 1. From LEFT to RIGHT: the diffusion function $\alpha(x, y)$, initial function $w^0 = w(x, y, 0)$ and beginning source function $\phi(w^0)(x, y)$. $h = 1/(m + 1)$, $m = 120$ are used.

on the Glowinski-Le Tallec splitting scheme (3.8), (3.9) will be developed and executed in multiple UNIX workstation platforms.

First of all, we show surfaces of the diffusion function $\alpha(x, y)$, initial function $w^0 = w(x, y, 0)$ and corresponding nonlinear source function $\phi(w^0)$ in Fig. 1. The dual sparking device and its impact to the source function are clearly visible. We particularly notice that

$$\max_{(x,y)\in\bar{\mathcal{D}}} w_0(x, y) = 0.0100, \quad \sup_{(x,y)\in\mathcal{D}} \phi(w_0)(x, y) \approx 1.01010101.$$

Though manual mesh refinements are practiced immediately before solution quenching, for the simplicity of illustration, simulation results will be presented primarily at fixed temporal locations according to the initial temporal step $0 < \tau \ll 1$ unless otherwise stated. Courant numbers ranging from 0.1 to 0.25 will be considered in experiments for better overall resolutions of singular quenching solutions. Standard numerical differentiations are used for evaluating derivatives.

We are particularly interested in the temporal derivative w_t since an alternative definition of quenching is that

$$\lim_{t\to T_\sigma^-} \sup_{(x,y)\in\mathcal{D}} w_t(x, y, t) = +\infty,$$

where $T_\sigma < \infty$ [6,14]. On the other hand, the nonlinear source function reflects the free energy level inside a combustor which is crucial to observe. To this end, Fig. 2 is designated for showing surfaces of the numerical solution w^n, its temporal derivative w_t^n, and corresponding nonlinear source function $\phi(w^n)$ at an early temporal level $n = 1000$. We may observe that the numerical solution well preserves the initial pattern of w_0 after a thousand temporal advancements. However, heights of its twin peaks are slightly elevated to $\max_{(x,y)\in\bar{\mathcal{D}}_h} w^{1000}(x, y) \approx 0.0162422042$. The surface pattern of w_t is particularly interesting which serves as an indication that the shape of function w is under a rapid change to a single peak formation with the peak located at the center of the domain $\mathcal{D}_h$ for quenching. For $n = 1000$ we also have $\max_{(x,y)\in\mathcal{D}_h} w_t^n(x, y) \approx 1.0552569929$ and $\max_{(x,y)\in\mathcal{D}_h} \phi(w^n)(x, y) \approx 1.0165103690$.

Continuing in Fig. 3, we show surface profiles of the numerical solution w^n, its temporal derivative w_t^n, and corresponding nonlinear source function $\phi(w^n)$ at the temporal level $n = 73000$ which is only few steps away from a quenching blow-up. It can be seen that the twin peaks of the solution have almost disappeared in this stage. The newly formed single peak formations of w^n, w_t^n and $\phi(w^n)$ indicate strongly not only a rapid increased fuel temperature in the combustion chamber, but also the fact that the combustion explosion must begin at a single location. These precisely agree with theoretical quenching predictions [1,6,19,25,28]. On the other hand, we may also observe that while the solution surface of w^n is relatively flat at the top and smooth, the rate of change function w_t^n and reaction function $\phi(w^n)$ become more much aggressive around

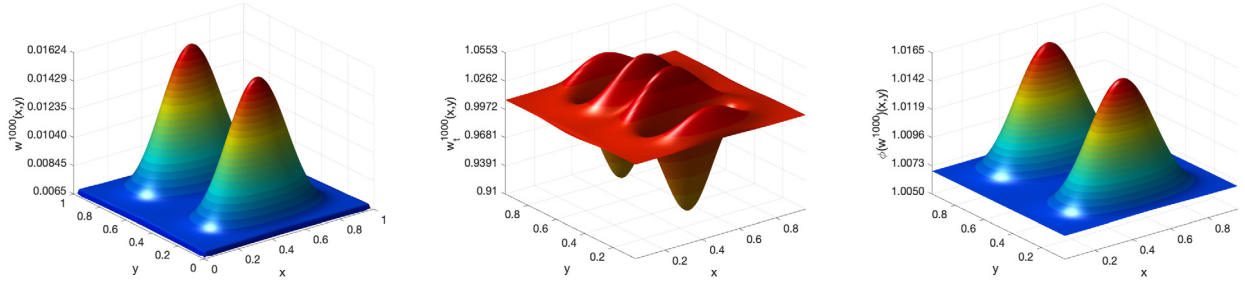

Fig. 2. From LEFT to RIGHT: the numerical solution w^{1000}, its temporal derivative w_t^{1000} and corresponding source function $\phi(w^{1000})$. The number of spacial grids used is $m = 120$, while a fixed Courant number $\kappa = 0.1$ is employed throughout computations.

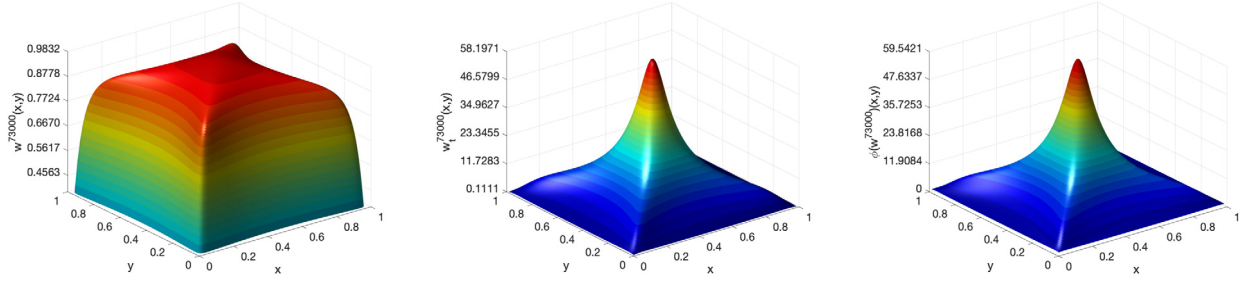

Fig. 3. From LEFT to RIGHT: the numerical solution w^{73000}, its temporal derivative w_t^{73000} and corresponding source function $\phi(w^{73000})$. The peak heights of $w^{73000}, w_t^{73000}, \phi(w^{73000})$ are approximately 0.98320516, 58.19712575 and 59.54210246, respectively. They are all located at the center of $\mathcal{D}_h$. Again, $m = 120$, $\kappa = 0.1$ are used.

Table 1
Highly monotone maximal values of the numerical solution w^n, its temporal derivative w_t^n and corresponding source function $\phi(w^n)$. Results are consistent with known solutions [3,6,17].

n	t	$\max_{\mathcal{D}_h} w^n$	$\max_{\mathcal{D}_h} w_t^n$	$\max_{\mathcal{D}_h} \phi(w^n)$
0	0	0.10	–	1.0101010101
1000	0.0068301345	0.0162422042	1.0552569929	1.0165103690
5000	0.0341506727	0.0424738757	1.0636412480	1.0443579289
10000	0.0683013455	0.0773479051	1.0958311366	1.0838321460
20000	0.1366026910	0.1528023112	1.1833344019	1.1803620492
30000	0.2049040366	0.2363253646	1.3091450296	1.3094581824
51000	0.3483368622	0.4534557616	1.8239738610	1.8296780570
65000	0.4439587459	0.6705877655	3.0115647032	3.0357099571
70000	0.4781094187	0.7979478447	4.8989724894	4.9492171907
73000	0.4985998224	0.9832051614	58.1971257534	59.5421024674
73009	0.4986612936	0.9873321444	76.4984581024	78.9399591092
33011	0.4986749538	0.9884478397	83.5553017850	86.5638959646
73013	0.4986886141	0.9896835442	93.0144008075	96.9325150625
73015	0.4987022744	0.9903606415	144998.701525573	103.741343630

the center of $\mathcal{D}_h$. Needless to say, the Glowinski-Le Tallec splitting algorithm (3.8), (3.9) shows a satisfactory stability and is highly accurate for capturing the quenching singularity and physical characteristics.

Fig. 4 is devoted to the last shot of the numerical approximation w^n, its rate of change function w_t^n and nonlinear source function $\phi(w^n)$ immediately before quenching at $n = 37015$. The peak values of $w^n, w_t^n, \phi(w^n)$ have reached $0.99036064, 1.44998701\times10^5$ and 1.03741343×10^2, respectively. Enlarged surface plots are shown in the subdomain $\{[0.4, 0.6] \times [0.4, 0.6]\} \cup \mathcal{D}_h \subset \mathcal{D}_h$ in the second row. We notice that the value of $\max_{(x,y)\in\mathcal{D}_h} w^n(x, y) \approx 0.9903606415$ is now significantly close to the dimensionless ignition temperature $\theta = 1$.

Maximal values of the numerical solution w^n, its rate-of-change function w_t^n and corresponding nonlinear source function $\phi(w^n)$ are given at selected temporal levels in Table 1. The table shows strong monotonically

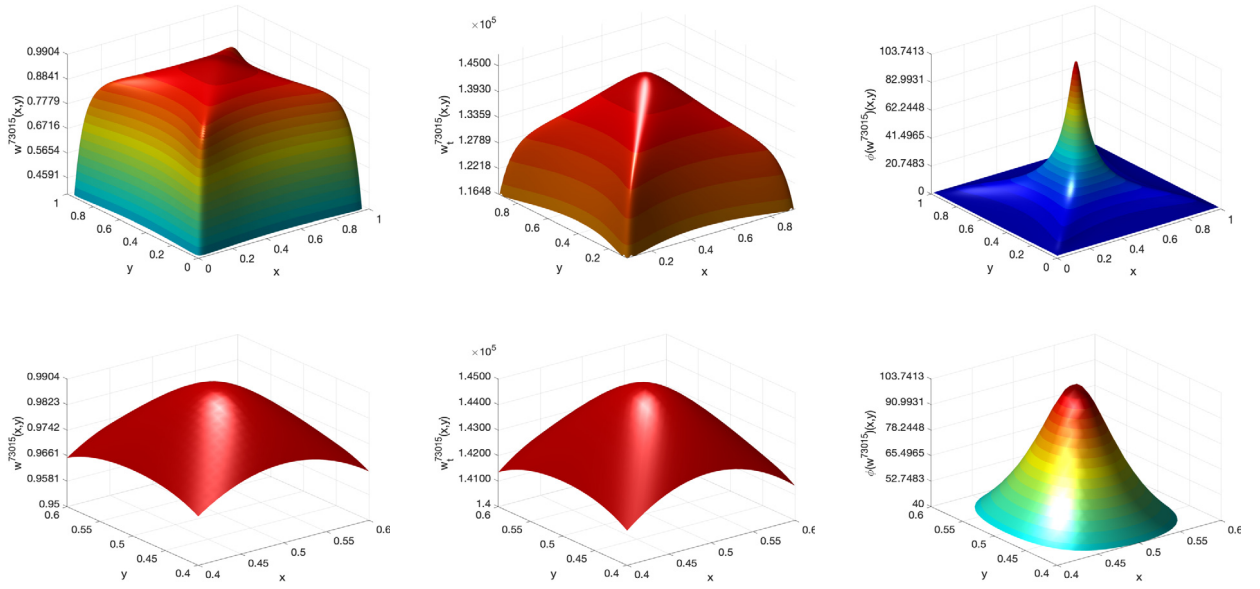

Fig. 4. From LEFT to RIGHT: the numerical solution w^{73015}, its temporal derivative w_t^{73015} and corresponding source function $\phi(w^{73015})$. In the bottom row enlarged simulations within the subdomain $\{[0.4, 0.6] \times [0.4, 0.6]\} \cup \mathcal{D}_h \subset \mathcal{D}_h$ are given. A typical single point quenching is evident.

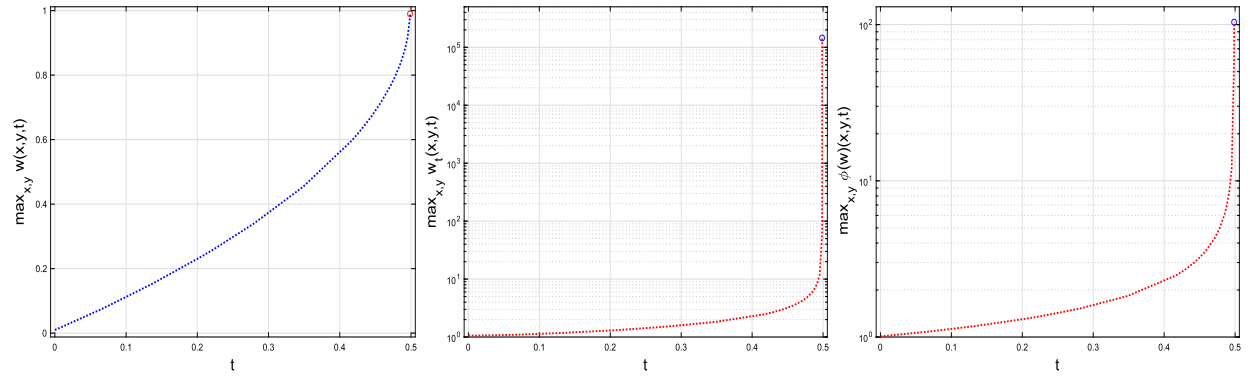

Fig. 5. Trajectories of the maximal values of the numerical solution w^n [LEFT], its temporal derivative w_t^n [MIDDLE] and nonlinear source function $\phi(w^n)$ [RIGHT]. The steadily increasing curves indicate a strong monotonicity of the functions. It may also be noticed that the maximal values of $w_t^n, \phi(w^n)$ begin to increase dramatically fast only as t enters the neighborhood of quenching time T_π. The phenomena are well consistent with those predicted by theoretical predictions [3,6,14,18,19].

increasing patterns of the data. It is noticed that $\max\limits_{(x,y)\in\mathcal{D}_h} w_t^{73015}(x,y) \approx 145000$ which is truly no surprise. Trajectories of the three targeted key functions are carefully illustrated in Fig. 5 until the quenching time $T_\pi \approx 0.4987022744$. Logarithmic scales are used in the y-direction to increase the readability. Both Table 1 and Fig. 5 show monotonically increasing structures of the targeted maximal values. Physically, these trajectories imply an ideal temperature built-up in the chamber from the initial fuel ignition to final combustion. The large number of temporal operations executed is a good indication of the superior numerical stability and reliability of the Glowinski-Le Tallec decomposition algorithm (3.8), (3.9) tested.

Now, let us computationally assess the order of convergence of the numerical solution. Apparently, a study of the convergence in temporal direction is sufficient since based on it, the spacial order of convergence can be derived conveniently via Courant constraints. To this end, we assume the following pointwise error estimate:

$$w(x_i, y_j, t_n) - w_{i,j}^n \approx C_0 \tau_n^p, \quad 1 \le i, j \le m,\ 0 < n \le N_\sigma, \tag{4.1}$$

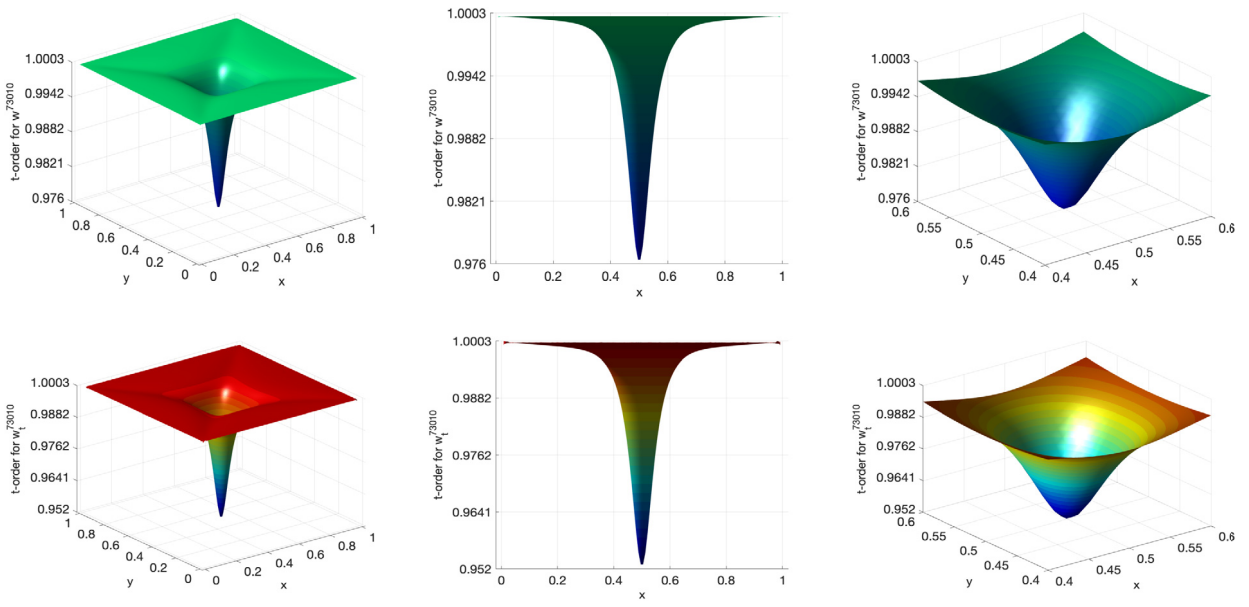

Fig. 6. TOP: computed temporal order of convergence for w^{73010}. BOTTOM: computed temporal order of convergence for the derivative function w_t^{73010}. From LEFT to RIGHT is the pointwise temporal order of convergence surfaces, projections of the surfaces to the XZ plane, and enlarged surface simulations within the subdomain $\{[0.4, 0.6] \times [0.4, 0.6]\} \cup \mathcal{D}_h$. The orders of convergence in both cases are approximately one, though they decay slightly in the quenching neighborhood which locates around the center of $\mathcal{D}$.

where $C_0 \in \mathbb{R}$ and $p = p_{i,j}^n$ is the order to be determined. Halve τ_n continuously. We obtain

$$w(x_i, y_j, t_n) - \hat{w}_{i,j}^{2n} \approx C_0(\tau_n/2)^p, \quad 1 \le i, j \le m,\ 0 < n \le N_\sigma, \tag{4.2}$$

$$w(x_i, y_j, t_n) - \tilde{w}_{i,j}^{4n} \approx C_0(\tau_n/4)^p, \quad 1 \le i, j \le m,\ 0 < n \le N_\sigma, \tag{4.3}$$

where the same indexes i, j are kept for the sake of simplicity in notations. A combination of (4.1)-(4.3) yields

$$p_{i,j}^n \approx \frac{1}{\ln 2} \ln \left| \frac{\hat{w}_{i,j}^{2n} - w_{i,j}^n}{\tilde{w}_{i,j}^{4n} - \hat{w}_{i,j}^{2n}} \right|, \quad 1 \le i, j \le m,\ 0 < n \le N_\sigma. \tag{4.4}$$

Replace the numerical solution by its temporal derivative in (4.1)-(4.4). We acquire the following pointwise temporal order of convergence for the derivative function w_t:

$$q_{i,j}^n \approx \frac{1}{\ln 2} \ln \left| \frac{(\hat{w}_t)_{i,j}^{2n} - (w_t)_{i,j}^n}{(\tilde{w}_t)_{i,j}^{4n} - (\hat{w}_t)_{i,j}^{2n}} \right|, \quad 1 \le i, j \le m,\ 0 < n \le N_\sigma. \tag{4.5}$$

Utilizing (4.4), (4.5), we may compute orders of convergence p^n, q^n pointwise at any temporal level $n > 0$. Since Kawarada equation solutions are particularly sensitive immediately before quenching, we show surfaces of p^n, q^n at $n = 73010$ in Fig. 6 as a benchmark illustration. We may observe that the surfaces are not only nonlinear but also reflecting precisely quenching singularities of the problem (3.1)-(3.3).

Furthermore, maximal, minimal, mean and median values of p^{73010}, q^{73010} are given in Table 2. It is evident that both orders of convergence are approximately one, though the former is in general slightly higher than the latter. The phenomena agree well with expectations from approximations [8,14,26]. Now, recall the weak Courant constraint $\tau_n/h^2 \in [\kappa - \epsilon, \kappa + \epsilon]$, where $\kappa \in \mathbb{R}^+$, $0 \le \epsilon < 1$ for $n = 0, 1, 2, \ldots, N_\sigma$. Therefore the convergence in space must be quadratic. This fact can be validated at any temporal level

Table 2
Benchmark values of the estimated temporal orders of convergence p^{73010}, q^{73010}, $(x, y) \in \mathcal{D}_h$.

Order of convergence	Maximal value	Minimal value	Mean value	Median value
p^{73010}	0.9999944610	0.9763945530	0.9992581732	0.9998565807
q^{73010}	1.0004187321	0.9529641787	0.9985614056	0.9997520193

$n \in \{1, 2, \ldots, N_\sigma\}$. Hence, the quadratic order of (3.8), (3.9) is preserved successfully by the Glowinski-Le Tallec splitting [11,16,30].

5. Concluding remarks

This paper shows that the Glowinski-Le Tallec splitting, which is originally introduced for computing global solutions of the equilibrium problems which are fundamental in Lagrangian optimizations, provides a consistent approximation to solutions of evolutional partial differential equations. The three-level, six-component decomposition is effective. It not only provides a generalization of conventional two-level, four-component ADI and LOD schemes, but also introduces a general way for constructing effective operator splitting methods. This means that products of operators such as $(I + \alpha_{k,\ell} t A_{r(k,\ell)})^{-1}$, $(I - \beta_{k,\ell} t A_{r(k,\ell)})$ in (1.1) instead of those via traditional Padé approximants [23,30,35], can be used as building blocks for highly flexible, and possibly higher order, splitting methods. The stability of the extended splitting method is experimented on a singular and nonlinear Kawarada problem for thermal engineering applications successfully. Pointwise quadratic convergence is assessed numerically.

The study and analysis also reveal that a continuing investigation of the Glowinski-Le Tallec splitting is necessary especially when solutions of other types of modeling equations, such as the degenerate stochastic Kawarada problems [17,25,26] and degenerate Lighthill-Whitham-Richards equations for polydisperse sedimentation and multiclass traffic dynamics [5,11], are considered. Approximations accepting nonpositive, or even complex, multiple parameters $\lambda_1, \lambda_2, \ldots, \lambda_M$ may be analyzed. Higher order operator decompositions beyond the basic Glowinski-Le Tallec splitting (1.4) must be researched. Split neural network structures also need to be implemented for methods overcoming the curse of dimensionality [9,11]. These are truly among our forthcoming expeditions to fulfill.

6. Appreciations

The author wishes to thank partial supports from the National Science Foundation (grant No. DMS-2318032; USA) and Simons Foundation (grant No. MPS-1001466; USA). The author also wishes to thank the editor and anonymous reviewers for their comments, suggestions and encouragements which help tremendously the improvement of this article.

References

[1] A.F. Acker, B. Kawohl, Remarks on quenching, Nonlinear Anal., Theory Methods Appl. 13 (1989) 53–61.
[2] H.H. Bauschke, P.L. Combettes, Convex Analysis and Monotone Operator Theory in Hilbert Spaces, Springer, Berlin, 2010.
[3] M. Beauregard, Q. Sheng, An adaptive splitting approach for the quenching solution of reaction-diffusion equations over nonuniform grids, J. Comput. Appl. Math. 241 (2013) 30–44.
[4] S. Blanes, F. Casas, A. Murua, Splitting methods in the numerical integration of non-autonomous dynamical systems, RACSAM 106 (2012) 49–66.
[5] S. Boscarino, R. Bürger, P. Mulet, G. Russo, L.M. Villada, Linearly implicit IMEX Runge-Kutta methods for a class of degenerate convection-diffusion problems, SIAM J. Sci. Comput. 37 (2) (2015) B305–B331.
[6] C.Y. Chan, L. Ke, Parabolic quenching for nonsmooth convex domains, J. Math. Anal. Appl. 186 (1994) 52–65.
[7] H. Cheng, P. Lin, Q. Sheng, R. Tan, Solving degenerate reaction-diffusion equations via variable step Peaceman-Rachford splitting, SIAM J. Sci. Comput. 25 (4) (2003) 1273–1292.
[8] S. Chin, Structure of positive decompositions of exponential operators, Phys. Rev. E 71 (2005) 016703.

[9] R. DeVore, B. Hanin, G. Petrova, Neural network approximation, Acta Numer. 30 (2021) 327–444.
[10] R. Gilmore, Baker-Campbell-Hausdorff formulas, J. Math. Phys. 15 (1974) 2090–2092.
[11] R. Glowinski, S.J. Osher, W. Yin, Splitting Methods in Communication, Imaging, Science, and Engineering, Springer, Berlin, 2017.
[12] G.H. Golub, C.F.V. Loan, Matrix Computations, 3rd edition, Johns Hopkins University Press, Baltimore and London, 1996.
[13] E. Hairer, A. Iserles, Numerical stability in the presence of variable coefficients, Found. Comput. Math. 16 (2016) 751–777.
[14] J.K. Hale, Asymptotic Behavior of Dissipative Systems, American Math Soc., Philadelphia, 1988.
[15] B. He, X. Yuan, On the convergence rate of Douglas-Rachford operator splitting method, Math. Program. 59 (2015) 715–722.
[16] A. Iserles, A First Course in the Numerical Analysis of Differential Equations, 2nd edition, Cambridge University Press, Cambridge and London, 2009.
[17] J. Kabre, Q. Sheng, A preservative splitting approximation of the solution of a variable coefficient quenching problem, Comput. Math. Appl. 100 (2021) 62–73.
[18] H. Kawarada, On solutions of initial-boundary value problems for $u_t = u_{xx} + 1/(1-u)$, Publ. Res. Inst. Math. Sci. 10 (1975) 729–736.
[19] H.A. Levine, Quenching, nonquenching, and beyond quenching for solution of some parabolic equations, Ann. Mat. Pura Appl. 155 (1989) 243–260.
[20] K. Liang, P. Lin, R. Tan, Numerical solution of quenching problems using mesh-dependent variable temporal steps, Appl. Numer. Math. 57 (2007) 791–800.
[21] P.L. Lions, B. Mercier, Splitting algorithms for the sum of two nonlinear operators, SIAM J. Numer. Anal. 16 (1979) 964–979.
[22] R.I. McLachlan, G.R.W. Quispel, Splitting methods, Acta Numer. 11 (2002) 341–434.
[23] C. Moler, C.F.V. Loan, Nineteen dubious ways to compute the exponential of a matrix, twenty-five years later, SIAM Rev. 45 (2003) 3–49.
[24] A. Moudale, On the convergence of splitting proximal methods for equilibrium problems in Hilbert spaces, J. Math. Anal. Appl. 359 (2009) 508–513.
[25] D. Nabongo, Quenching for semidiscretizations of a heat equation with a singular boundary condition, Asymptot. Anal. 16 (2008) 27–38.
[26] J.L. Padgett, Q. Sheng, Numerical solution of degenerate stochastic Kawarada equations via a semi-discretized approach, Appl. Math. Comput. 325 (2018) 210–226.
[27] D.W. Peaceman, H.H. Rachford, The numerical solution of parabolic and elliptic differential equations, J. Soc. Ind. Appl. Math. 43 (1955) 28–41.
[28] T. Poinset, D. Veynante, Theoretical and Numerical Combustion, 2nd edition, Edwards Publisher, Philadelphia, 2005.
[29] Q. Sheng, Solving linear partial differential equations by exponential splitting, IMA J. Numer. Anal. 9 (1989) 199–212.
[30] Q. Sheng, The ADI method, in: B. Engquist (Ed.), Encyclopedia of Applied and Computational Mathematics, Springer, Heidelberg, 2015, pp. 25–33.
[31] M. Suzuki, General theory of fractal path integrals with applications to many-body theories and statistical physics, J. Math. Phys. 32 (1991) 400–407.
[32] H.F. Trotter, On the product of semi-groups of operators, Proc. Am. Math. Soc. 10 (1959) 545–551.
[33] E.H. Twizell, Y. Wang, W.G. Price, Chaos-free numerical solutions of reaction-diffusion equations, Proc. Royal Soc. London Sect. A 430 (1991) 541–576.
[34] P.T. Vuong, J.J. Strodiot, The Glowinski-Le Tallec splitting method revisited in the framework of equilibrium problems in Hilbert spaces, J. Glob. Optim. 70 (2018) 477–495.
[35] N.N. Yanenko, The Method of Fractional Steps; the Solution of Problems of Mathematical Physics in Several Variables, Springer, Berlin, 1971.